

Evidence for Solution-State Nonlinearity of sp-Carbon Chains Based on IR and Raman Spectroscopy: Violation of Mutual Exclusion

Andrea Lucotti,[†] Matteo Tommasini,[†] Daniele Fazzi,[†] Mirella Del Zoppo,[†] Wesley A. Chalifoux,[‡] Michael J. Ferguson,[‡] Giuseppe Zerbi,^{*,†} and Rik R. Tykwinski^{*,‡}

Politecnico di Milano, Dipartimento di Chimica, Materiali e Ingegneria Chimica "G. Natta" Piazza Leonardo da Vinci 32, 20133 Milano, Italy, and Department of Chemistry, University of Alberta, Edmonton, Alberta, Canada T6G 2G2

Received October 26, 2007; E-mail: giuseppe.zerbi@polimi.it; rik.tykwinski@ualberta.ca

Abstract: Adamantyl-end-capped polyynes with chains of 4, 6, 8, 10, 12, 16, and 20 sp-hybridized carbons (**C4–C20**) have been synthesized and their IR and Raman spectra obtained. On the basis of violations of the mutual-exclusion principle between IR and Raman spectroscopy, spectral evidence demonstrates that these molecules possess a noncentrosymmetric molecular structure in both the solid and solution states. This premise is supported by X-ray crystallographic analysis of **C12**, which shows a bent, noncentrosymmetric structure in the solid state. Density functional theory (DFT) calculations for adamantyl-end-capped polyynes, in comparison with those for hydrogen-end-capped polyynes, show that the observed violation of mutual exclusion is independent of the end group of the polyyne chain (i.e., adamantyl versus H). The origin of these experimental spectroscopic observations is ascribed to the existence of dynamic contributions to molecular nonlinearity resulting from low-frequency skeletal bending vibrations of the chains and/or the existence of low-energy bent conformations of the polyyne chains, as DFT-optimized structures seem to suggest.

Introduction

sp-Hybridized carbon chains composed of alternating single and triple bonds (polyynes)¹ are found in interstellar space, plants, fungi, and marine organisms.² Polyynes are also used extensively as building blocks for materials and supramolecular chemistry.³ While polyynes are commonly assumed to be "linear" molecules, X-ray crystallographic analyses have shown

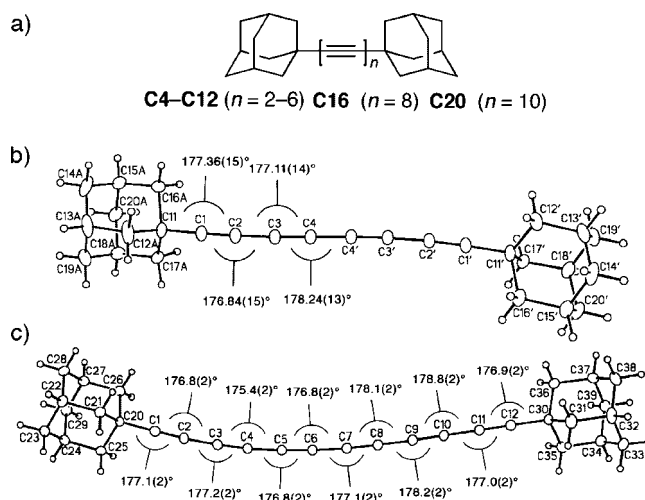


Figure 1. (a) Chemical structures of **C4–C20**. ORTEP drawings of (b) **C8** and (c) **C12** in the solid state, as derived from X-ray diffraction studies.

that these molecules often display considerable static nonlinearity in the solid state.^{4–6} This is demonstrated in Figure 1, where the solid-state structures of polyynes **C8** and **C12** show

(6) For theoretical studies of bending, see: (a) Maier, W. F.; Lau, G. C.; McEwen, A. B. *J. Am. Chem. Soc.* **1985**, *107*, 4724–4731. (b) Santiago, C.; Houk, K. N.; DeCicco, G. J.; Scott, L. T. *J. Am. Chem. Soc.* **1978**, *100*, 692–696.

[†] Politecnico di Milano.

[‡] University of Alberta.

- (1) The term polyyne is used here to describe molecules that contain two or more conjugated triple bonds.
- (2) (a) Shi Shun, A. L. K.; Tykwinski, R. R. *Angew. Chem., Int. Ed.* **2006**, *45*, 1034–1057. (b) *Polyynes: Synthesis, Properties, and Applications*; Cataldo, F., Ed.; Taylor & Francis: Boca Raton, FL, 2006. (c) Bohlmann, F.; Burkhardt, T.; Zdero, C. *Naturally Occurring Acetylenes*; Academic Press: New York, 1973.
- (3) (a) *Acetylene Chemistry: Chemistry, Biology, and Material Science*; Diederich, F.; Stang, P. J.; Tykwinski, R. R., Eds.; Wiley-VCH: Weinheim, Germany, 2005. (b) *Carbon-Rich Compounds*; Haley, M. M.; Tykwinski, R. R., Eds.; Wiley-VCH: Weinheim, Germany, 2006; Chapter 6.
- (4) Szafert, S.; Gladysz, J. A. *Chem. Rev.* **2006**, *106*, PR1–PR33.
- (5) (a) Eisler, S.; Slepkov, A. D.; Elliott, E.; Luu, T.; McDonald, R.; Hegmann, F. A.; Tykwinski, R. R. *J. Am. Chem. Soc.* **2005**, *127*, 2666–2676. (b) Luu, T.; Elliott, E.; Slepkov, A. D.; Eisler, S.; McDonald, R.; Hegmann, F. A.; Tykwinski, R. R. *Org. Lett.* **2005**, *7*, 51–54. (c) Dembinski, R.; Lis, T.; Szafert, S.; Mayne, C. L.; Bartik, T.; Gladysz, J. A. *J. Organomet. Chem.* **1999**, *578*, 229–246. (d) Mohr, W.; Stahl, J.; Hampel, F.; Gladysz, J. A. *Chem.—Eur. J.* **2003**, *9*, 3324–3340. (e) Antonova, A. B.; Bruce, M. I.; Elis, B. G.; Gaudio, M.; Humphrey, P. A.; Jevric, M.; Melino, G.; Nicholson, B. K.; Perkins, G. J.; Skelton, B. W.; Stapleton, B.; White, A. H.; Zaitseva, N. N. *Chem. Commun.* **2004**, 960–961.

bond angles ranging from 175 to 179°, as determined by X-ray crystallography.⁷ Other sp-carbon chains, such as, for example, carbon suboxide⁸ and carbon clusters,⁹ have been shown experimentally to possess shallow bending potentials in the gas phase. Additionally, the existence of a nonlinear equilibrium structure or shallow bending potential has also been computationally predicted for some cumulenes,¹⁰ small carbon-clusters,^{9,11} and carbon suboxide.¹² From an experimental point of view, gas-phase bending (static and/or dynamic) of carbon chains and clusters is also expected to play a dominant role in fullerene formation.^{9,13}

The question that remains to be answered concerns the structure of polyynes in solution, where the influence of end groups and the associated “crystal packing effects” that dominate in the solid state should be absent. The tendency of polyynes to adopt a nonlinear geometry (static and/or dynamic) in the solution state would suggest that a bent structure is an intrinsic characteristic of the molecules rather than a simple consequence of crystal packing observed in the solid state. To date, however, experimental evidence that might substantiate the nonlinearity of polyynes in solution has not, to our knowledge, been reported.

It is well-established¹⁴ that the noncoincidence of Raman and IR spectra (the so-called mutual-exclusion principle) provides unquestionable experimental evidence of a centrosymmetric molecular structure. On the basis of Raman and IR spectroscopy, the present study shows a violation of mutual exclusion for polyynes in both the solution and solid states. This suggests that the adamantyl-end-capped polyynes lack inversion symmetry in solution and therefore are not inherently linear, particularly in the case of longer chains. This supposition is also supported by density functional theory (DFT) calculations.

The nonlinear shape of longer polyynes in the solution state can reasonably be ascribed to the existence of low-energy bent conformers (static nonlinearity) and/or the shallowness of the bending potential of the sp-carbon chains (dynamic nonlinearity).¹⁵ Given a shallow bending potential and/or low-energy

nonlinear conformers, large-amplitude bending motions of the polyyne chain are expected at room temperature in the solution state, and the thermal excitation of low-energy bending vibrations should be substantial. The time scale of these low-energy bending vibrations is $\sim 1/40$ that of C≡C stretching vibrations.^{16a,b} Thus, as the C≡C stretches are probed experimentally by IR and Raman analysis in the 2000 cm⁻¹ region, the chain molecule is found in a nonlinear, noncentrosymmetric geometry, as established by the observed violation of mutual exclusion. Effectively, this situation is best described as a “dynamic symmetry breaking” that can be probed by examination of the high-frequency C≡C stretching modes. DFT calculations carried out on model bent molecules confirm that even a slight distortion of the polyyne chain to a noncentrosymmetric structure should provide an experimentally observable loss of the IR/Raman mutual-exclusion in the 2000 cm⁻¹ region.

Results and Discussion

Solid-State Analysis. Examination of the Raman spectra of polyynes **C4–C20** in their crystalline states shows that these spectra are very clean, and the strongest lines observed in the 1950–2300 cm⁻¹ range are unquestionably assigned^{17a–c} to the \mathcal{A} mode in the frame of the effective conjugation coordinate (ECC) theory^{17d,e} of polyconjugated chains (Figure 2a).¹⁸ All of the other lines found in the spectra can be assigned to the adamantyl groups,¹⁹ except for a few minor lines below 600 cm⁻¹ that are assigned to transverse and/or longitudinal vibrational modes of the polyyne chains.^{16c,20} As expected from the ECC model, a decrease in the Raman frequency of the \mathcal{A} mode is observed as the number of C≡C bonds increases in going from **C4** (2250 cm⁻¹) to **C20** (1950 cm⁻¹), as shown in Table 1.^{17b,21}

Examination of the solid-state IR spectra shows that while **C6–C10** exhibit only a single absorption each, two significant IR absorptions are found for each of the longer adamantyl-end-capped polyynes **C12–C20** in the spectral region ascribed to

- (7) Adamantyl-end-capped **C4–C20** were synthesized using a modified Fritsch–Buttenberg–Wiechell (FBW) rearrangement analogous to that reported in ref 5a,b (see the Supporting Information for synthetic and crystallographic details). For other recent examples of polyyne formation using the FBW rearrangement, see: (a) Chalfoux, W. A.; Tykwinski, R. R. *Chem. Rec.* **2006**, *6*, 169–182. (b) Eisler, S.; Chahal, N.; McDonald, R.; Tykwinski, R. R. *Chem.–Eur. J.* **2003**, *9*, 2542–2550. (c) Tobe, Y.; Umeda, R.; Iwasa, N.; Sonoda, M. *Chem.–Eur. J.* **2003**, *9*, 5549–5559.
- (8) Masiello, T.; Voorhees, A. J.; Abel, M. J.; Nibler, J. W. *J. Phys. Chem. A* **2005**, *109*, 3139–3145.
- (9) Van Orden, A.; Saykally, R. J. *Chem. Rev.* **1998**, *98*, 2313–2357.
- (10) Liang, C.; Allen, L. C. *J. Am. Chem. Soc.* **1991**, *113*, 1873–1878.
- (11) Botschwina, P. *J. Phys. Chem. A* **2007**, *111*, 7431–7436.
- (12) Koput, J. *Chem. Phys. Lett.* **2000**, *320*, 237–244.
- (13) (a) Faust, R. *Angew. Chem., Int. Ed.* **1998**, *37*, 2825–2828. (b) Goroff, N. S. *Acc. Chem. Res.* **1996**, *29*, 77–83. (c) Kiang, C. H.; Goddard, W. A. *Phys. Rev. Lett.* **1996**, *76*, 2515–2518. (d) Hunter, J. M.; Fye, J. L.; Roskamp, E. J.; Jarrold, M. F. *J. Phys. Chem.* **1994**, *98*, 1810–1818. (e) Weltner, W.; Vanzee, R. J. *Chem. Rev.* **1989**, *89*, 1713–1747.
- (14) Herzberg, G. *Molecular Spectra and Molecular Structure*, Vol. 2; D. Van Nostrand: Princeton, NJ, 1945.
- (15) In order to settle this point from a theoretical perspective, however, very accurate correlated methods are needed, as work with carbon suboxide and other linear sp-carbon clusters has nicely demonstrated.^{8–12} Given that current DFT methods are not likely to meet the strict requirements for accuracy necessary for the detailed study of the polyyne bending potential, the DFT calculations reported here aim primarily at the assignment of the fundamental C≡C stretching lines observed in the IR and Raman spectra. This analysis successfully demonstrates that through a realistic bending of the chain, a detectable violation of mutual exclusion is produced.

- (16) (a) Neugebauer, J.; Reiher, M. *J. Phys. Chem. A* **2004**, *108*, 2053–2061. (b) Zahradnik, R.; Sroubkova, L. *Helv. Chim. Acta* **2003**, *86*, 979–1000. (c) Casari, C. S.; Li Bassi, A.; Baserga, A.; Ravagnan, L.; Piseri, P.; Lenardi, C.; Tommasini, M.; Milani, A.; Fazzi, D.; Bottani, C. E.; Milani, P. *Phys. Rev. B* **2008**, *77*, 195444.
- (17) (a) Milani, A.; Tommasini, M.; Del Zoppo, M.; Castiglioni, C.; Zerbi, G. *Phys. Rev. B* **2006**, *74*, 153418. (b) Tommasini, M.; Fazzi, D.; Milani, A.; Del Zoppo, M.; Castiglioni, C.; Zerbi, G. *J. Phys. Chem. A* **2007**, *111*, 11645–11651. (c) Tommasini, M.; Milani, A.; Fazzi, D.; Del Zoppo, M.; Castiglioni, C.; Zerbi, G. *Physica E* **2008**, *40*, 2570–2576. (d) Castiglioni, C.; Zerbi, G.; Gussoni, M.; Lopez Navarrete, J. T. *Solid State Commun.* **1988**, *65*, 625–630. (e) Castiglioni, C.; Tommasini, M.; Zerbi, G. *Philos. Trans. R. Soc. London, Ser. A* **2004**, *362*, 2425–2459.
- (18) Extensive theoretical work and first-principles calculations support the premise that the strong Raman band (\mathcal{A} mode) considered here (and activated in the IR spectrum) is certainly a fundamental vibration rather than a combination or Fermi resonance band (see ref 17).
- (19) Jensen, J. O. *Spectrochim. Acta, Part A* **2004**, *60*, 1895–1905.
- (20) Anharmonicity is expected to play a major role in the description of low-frequency bending vibrations but should not affect the selection rules for the fundamental vibrations (\mathcal{A} band) discussed here. More specifically, anharmonicity certainly changes the vibrational wave function, but it cannot change the irreducible representation to which it belongs. In other words, selection rules for fundamentals are not expected to be broken if anharmonicity is taken into account; only the value of the transition probabilities would be affected. While anharmonicity is considered to be weak and negligible for the high-frequency C≡C stretching vibrations explored in this study, it is expected to play a major role in the description of the low-frequency bending vibrations. This discussion is, however, outside the scope of the current investigation. For a theoretical description of anharmonicity effects in polyynes, see ref 16a.

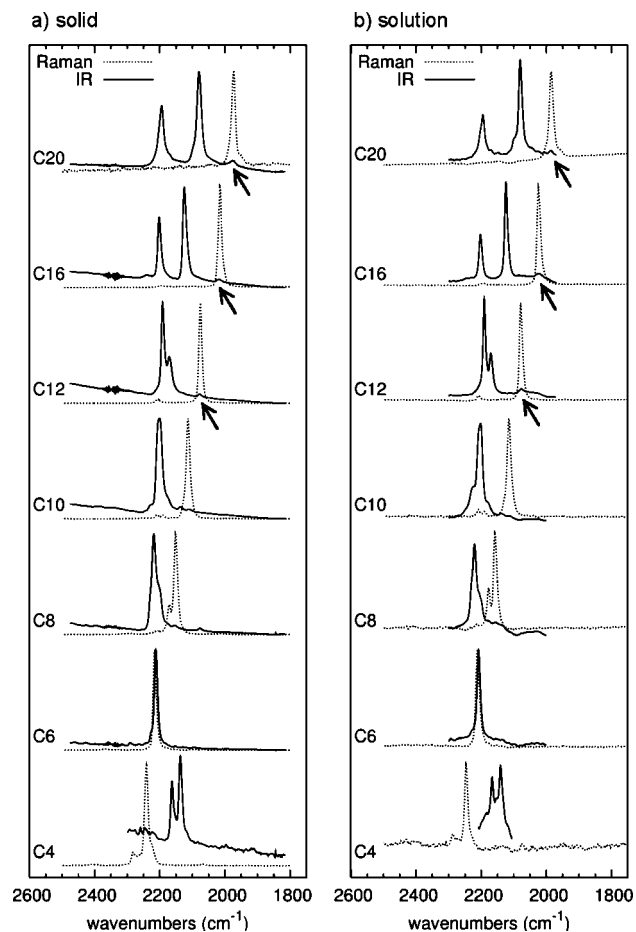


Figure 2. (a) Experimental Raman (····) and IR (—) spectra (2500–1800 cm^{-1}) of (a) solid samples and (b) THF solutions of polyynes **C4–C20**. The arrows indicate violations of mutual exclusion in the IR spectra.

$\text{C}\equiv\text{C}$ stretching.²² Calculations show that the two observed IR bands can be assigned to \mathcal{A} modes that differ in the number of nodes of the vibrational displacements of the chain (longitudinal, one-dimensional confined phonons; see Figure 3). The spectra show frequency dispersion for one of the IR-active \mathcal{A} modes, which decreases in energy as the chain length increases (Figures 2 and 3). The other IR band maintains approximately the same frequency irrespective of the polyne length.

According to group theory, for centrosymmetric systems, the Raman-active \mathcal{A} -mode vibrations are totally symmetric (*g*, gerade) and the IR-active lines antisymmetric (*u*, ungerade) with respect to the center of symmetry of the molecule. From a comparison of the solid-state spectra in Figure 2a (see arrows),

- (21) For exemplary studies of polyynes by Raman spectroscopy, see: (a) Schermann, G.; Grösser, T.; Hampel, F.; Hirsch, A. *Chem.–Eur. J.* **1997**, *3*, 1105–1112. (b) Dembinski, R.; Bartik, T.; Bartik, B.; Jaeger, M.; Gladysz, J. A. *J. Am. Chem. Soc.* **2000**, *122*, 810–822. (c) Tabata, H.; Fujii, M.; Hayashi, S.; Doi, T.; Wakabayashi, T. *Carbon* **2006**, *44*, 3168–3176. (d) Lucotti, A.; Tommasini, M.; Del Zoppo, M.; Castiglioni, C.; Zerbi, G.; Cataldo, F.; Casari, C. S.; Li Bassi, A.; Russo, V.; Bogana, M.; Bottani, C. E. *Chem. Phys. Lett.* **2006**, *417*, 78–82. (e) Yang, S.; Kertesz, M.; Zólyomi, V.; Kürti, J. *J. Phys. Chem. A* **2007**, *111*, 2434–2441. (f) Casari, C. S.; Russo, V.; Li Bassi, A.; Bottani, C. E.; Cataldo, F.; Lucotti, A.; Tommasini, M.; Del Zoppo, M.; Castiglioni, C.; Zerbi, G. *Appl. Phys. Lett.* **2007**, *90*, 013111. (g) Milani, A.; Tommasini, M.; Fazzi, D.; Castiglioni, C.; Del Zoppo, M.; Zerbi, G. *J. Raman Spectrosc.* **2008**, *39*, 164–168.
- (22) The IR spectra of **C4** show a doublet in the $\text{C}=\text{C}$ stretching region, which can be assigned to a Fermi resonance with a CH bending vibration (see the Supporting Information).

it is clear that perfect mutual exclusion between the Raman and IR lines is not upheld, particularly for the longer polyynes **C12–C20**. The totally symmetric Raman-active \mathcal{A} -mode lines at 2075, 2014, and 1974 cm^{-1} for **C12**, **C16**, and **C20**, respectively, are also conspicuously present as weak features in the corresponding IR spectra. It can thus be concluded that the longer polyynes have an equilibrium structure in the solid state in which the molecule lacks inversion symmetry.

This finding is not especially surprising, since the inversion symmetry of a linear chain is lost when it is bent into a bowl-like shape, a feature often documented by X-ray diffraction studies of polyynes,⁴ including **C12** (Figure 1c), where the noncentrosymmetric structure shows $\text{C}-\text{C}\equiv\text{C}$ bond angles in the range $175.4(2)$ – $178.8(2)^\circ$ with an average of 177.2° . Thus, the lack of an inversion center for **C12** in the solid state accounts for the experimental IR and Raman observations. It might be noted that the “static” bent geometry observed for crystalline **C12** does not exclude, even in the solid state, a contribution to the observed noncoincidence by a “dynamical disorder” due to a shallow bending potential, as discussed in the Introduction.

In the search for a rationalization of these experimental observations, it may be argued that the centrosymmetric structure of the adamantyl-end-capped polyynes is most easily destroyed if the terminal adamantyl groups adopt an eclipsed conformation, which might then give rise to the weak IR bands observed in the Raman spectra. This premise is not, however, consistent with the observed data. Specifically, the adamantyl–adamantyl interaction of the eclipsed conformation should be stronger in the shorter polyynes because of the smaller separation between the end groups. On the contrary, the longer polyne chains **C12–C20** experimentally show a more definite activation of the Raman mode in the IR spectrum. Moreover, first-principles calculations for $\text{H}-(\text{C}\equiv\text{C})_5-\text{H}$, the hydrogen-terminated parent polyne of **C10**, demonstrate the analogous violation of mutual exclusion (see below).²³ This suggests that the nature of the end group is seemingly irrelevant.

Solution-State Analysis. Unfortunately, no structural information is readily available for the carbon chains in solution. The observation of the lack of mutual exclusion between Raman and IR spectra recorded on solutions represents the first reported attempt, outside of gas-phase analyses, to characterize the shape of polyne chains in the absence of crystal-field effects and/or effects due to solid-state packing of end groups.

The gross features of the IR and Raman spectra of **C4–C20** measured in THF solution (Figure 2b) are remarkably similar in nearly all respects to those measured in the solid state. This includes the presence of strong Raman-active ∞ -mode lines that decrease in frequency as the chain length increases in going from **C4** (2246 cm^{-1}) to **C20** (1985 cm^{-1}) and two IR-active transitions, one of which shifts to lower frequency as the polyne length increases. The only major difference between the solution- and solid-state spectra is a small, nonsystematic frequency shift in both the IR and Raman values recorded for the solution state relative to those for the solid state. These small variances between phases are commonly encountered in spectroscopy and arise from effects of the molecular environment.

The analysis of the solution-state spectra shows that for polyynes **C12–C20**, mutual exclusion between the Raman and IR spectra is not upheld. In particular, the totally symmetric Raman-active \mathcal{A} -mode lines at 2078, 2024, and 1985 cm^{-1} for

- (23) A similar violation of mutual exclusion is also found in bent $\text{H}-(\text{C}\equiv\text{C})_6-\text{H}$ (see the Supporting Information).

Table 1. Experimental Solution- and Solid-State Raman and IR Frequencies for Polyynes β -Mode Lines^a

	solid-state frequencies (cm ⁻¹)		solution-state frequencies (cm ⁻¹)	
	Raman	IR	Raman	IR
C4	2241 s	2163 s, 2137 s	2246 s	2166 s, 2141 s
C6	2216 s	2212 s	2211 s	2208 s
C8	2171 m, 2151 s	2218 s	2177 m, 2158 s	2220 s
C10	2113 s	2201 s	2115 s	2204 s
C12	2075 s	2191 s, 2171 s, 2078 w	2078 s	2191 s, 2170 s, 2078 w
C16	2014 s	2202 s, 2125 s, 2018 w	2024 s	2203 s, 2124 s, 2024 w
C20	1974 s	2194 s, 2080 s, 1976 w	1985 s	2195 s, 2081 s, 1985 w

^a Intensity labels: s, strong; m, medium; w, weak.

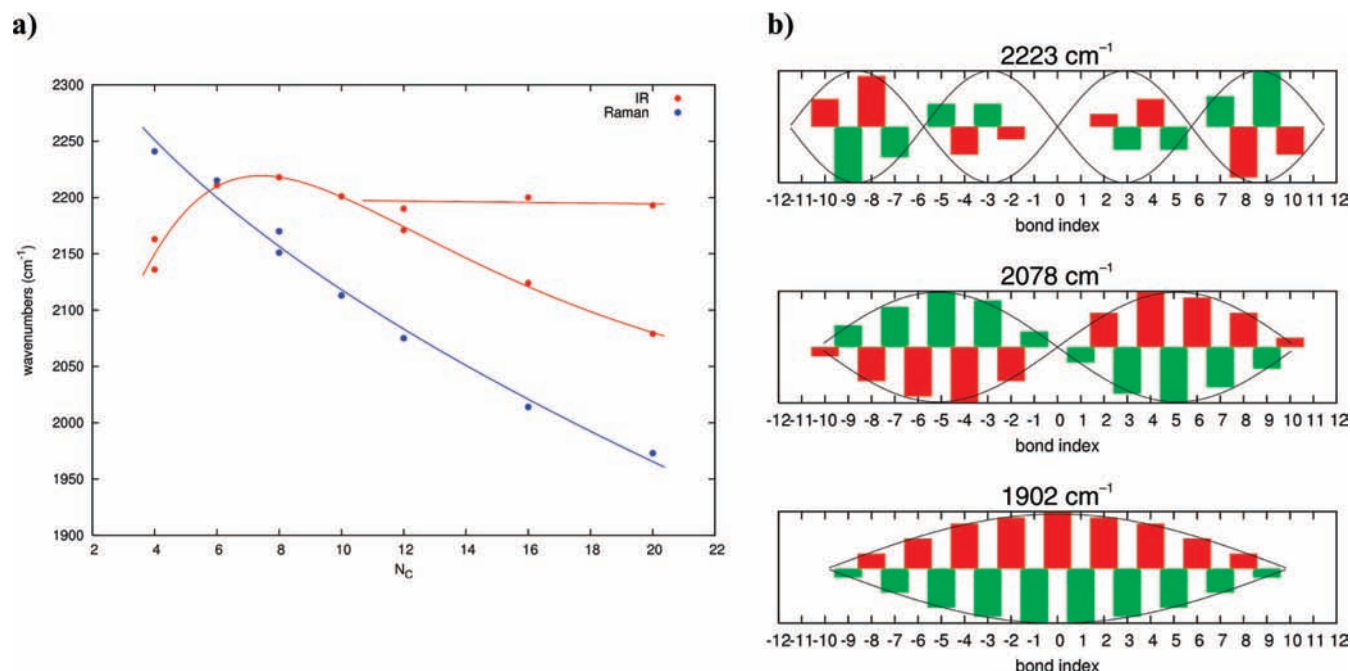


Figure 3. (a) Experimental frequency dispersion of Raman and IR lines as a function of the number of carbon atoms (from spectroscopic data in the solid state). (b) Theoretical vibrational displacements (bond-length changes) for **C20** associated with the three branches of the plot in (a) (from PBE/PBE/cc-pVDZ calculations). Unscaled theoretical vibrational frequencies are also given. The central bond of the chain is indicated by the bond index of zero. Green bars denote C=C bonds and red bars C-C bonds. Sinusoidal lines are superimposed onto the stick plots to ease the recognition of the number of nodes.

C12, **C16**, and **C20**, respectively, are also present in the corresponding IR spectra at essentially identical frequencies. These data thus confirm that (a) at least locally, a noncentrosymmetric polyynes chain is present in solution and (b) the nonlinear geometry is related to the intrinsic nature of polyynes, i.e., it is determined by the shallowness of the intramolecular potential along C-C≡C bending coordinates.

Computational Analysis. On the basis of the above discussion, the following questions need further consideration: (a) Is the static equilibrium geometry of polyynes bent or linear? (b) Is the polyynes bending potential indeed very shallow? (c) Can only a slightly bent polyynes framework account for the non-negligible spectroscopic observations of the breakdown of mutual exclusion (i.e., Raman modes activated in the IR spectrum)? (d) Do the end groups (e.g., adamantyl) significantly affect the experimental symmetry considerations presented? (e) Is it possible that the IR signals ascribed to the violation of mutual exclusion arise from an ungerade IR-active vibration of similar frequency? DFT calculations can help with the answers to these questions, and several sets of calculations were undertaken. First, DFT simulations using the pure PBE²⁴ functional and Dunning's double- ζ

correlation-consistent cc-pVDZ basis set²⁵ were carried out on **C4**–**C20** to model the structures, bond lengths, and bond angles of these molecules. The computational procedure started from an initially bent polyynes skeleton, and for longer chains (**C12**–**C20**), the geometry optimization converged to a slightly bent structure as a minimum. Previous experimental^{8,9} and theoretical^{10–12} studies agree that the bending potential of related linear carbon structures is shallow. As for the presence of stable minima for bent structures, recent work has shown that this seems to be the case in carbon suboxide^{8,12} and Pt-end-capped polyynes.²⁶ Thus, the overall bent shape calculated for the adamantyl-end-capped polyynes could result from either a very flat minimum corresponding to the linear structure or a stable minimum for a bent geometry.²⁷

To more fully assess the prospect of a nonlinear ground-state structure for the adamantyl polyynes and the associated vibra-

(24) Perdew, J. P.; Burke, K.; Ernzerhof, M. *Phys. Rev. Lett.* **1996**, *77*, 3865–3868.

(25) Woon, D. E.; Dunning, T. H., Jr. *J. Chem. Phys.* **1993**, *98*, 1358–1371.

(26) Zhuravlev, F.; Gladysz, J. A. *Chem.—Eur. J.* **2004**, *10*, 6510–6522.

(27) A comparison of the theoretical results for carbon suboxide described in refs 8 and 12 clearly demonstrates the need for higher-level calculations in such analyses. Explicit and accurate inclusion of electron correlation is crucial for obtaining good results for the bending potential, even for carbon suboxide and other sp-carbon chains (see ref 11).

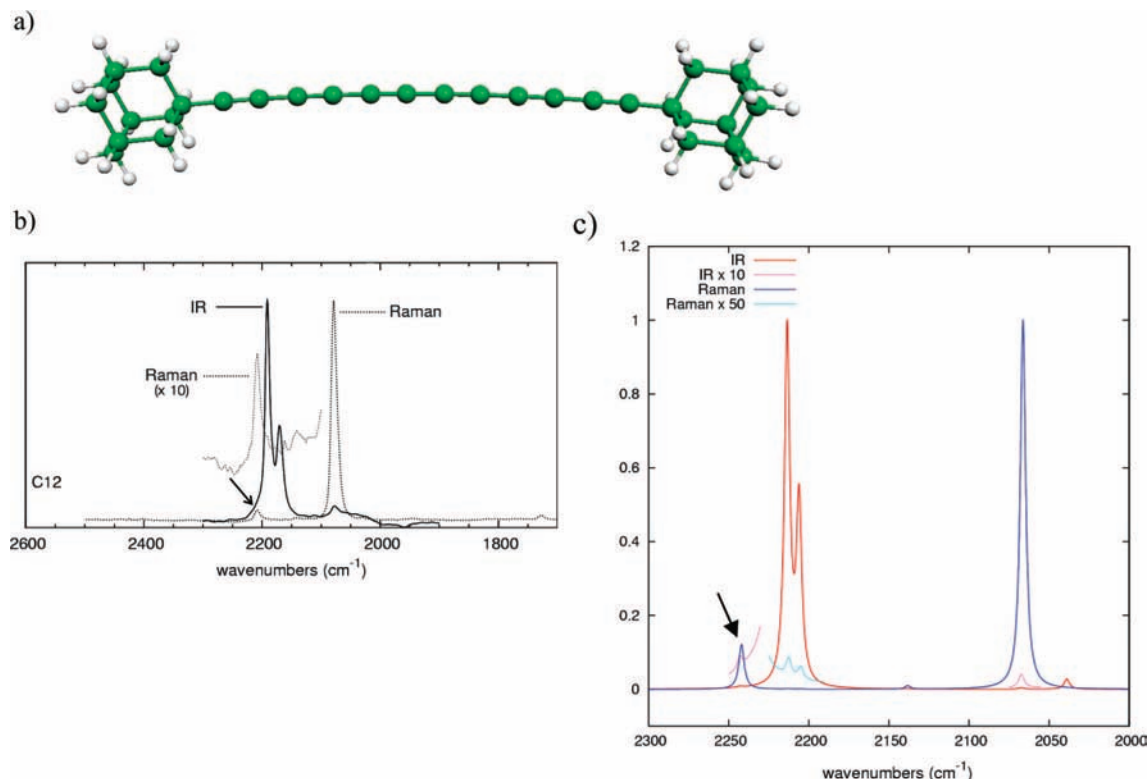


Figure 4. (a) Ball-and-stick model of the optimized bent structure of **C12** calculated from first principles (PBEPBE/cc-pVDZ). (b) Experimental IR and Raman spectra of **C12** in THF solution. (c) Simulated IR and Raman spectra of **C12** based on first-principles calculations at the PBEPBE/cc-pVDZ level. The arrows in (b) and (c) denote a Raman mode activated in the IR spectrum, as predicted by the calculations.

tional analysis, additional first-principles calculations (PBEPBE/cc-pVDZ) for **C12** were carried out (Figure 4a). This analysis supports a bent structure for **C12**. Furthermore, the calculated IR and Raman spectra (Figure 4c) compare fairly well with the experimental observations in the $\text{C}\equiv\text{C}$ stretching region (Figure 4b). An analysis of the simulations of the Raman and IR spectra shows that the mutual-exclusion principle is violated not only in the IR spectrum but also in the Raman spectrum.²⁸ Moreover, the violation of mutual exclusion is predicted in the IR spectrum for a second band (see the arrow in Figure 4c) in addition to the ECC band. These calculations support the assignment of the observed shoulder in the IR spectrum to a Raman mode activated in the IR spectrum (see corresponding arrow in the experimental spectrum in Figure 4b).

To confirm that the results for polyynes **C4–C20** did not arise from an end-group effect generated by the adamantyl groups, first-principles calculations were carried out at the PBEPBE/cc-pVQZ level for the parent pentayne $\text{H}-(\text{C}\equiv\text{C})_5-\text{H}$ for both linear and bent conformations (Figure 5).²⁹ It is worth noting that in this case, a more extended basis set (quadruple- ζ as opposed to double- ζ) was used in view of the simpler molecular structure (i.e., no terminal adamantyl groups). The results confirm a detectable activation in the IR spectrum of the strong Raman band as well as the converse, i.e., activation in the Raman spectrum of the strong IR band. These calculations

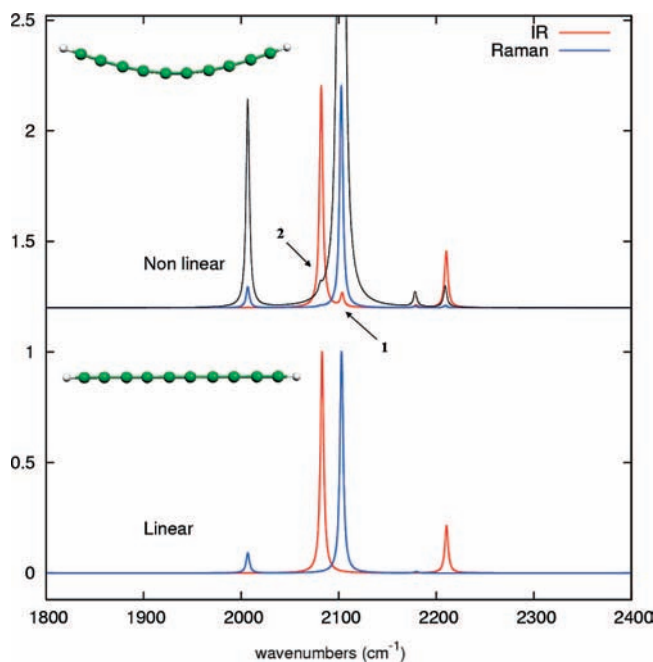


Figure 5. Simulated Raman and IR spectra of the (top) bent and (bottom) linear conformations of $\text{H}-(\text{C}\equiv\text{C})_5-\text{H}$ calculated at the PBEPBE/cc-pVQZ level (the simulated structures are shown as insets). The thin black curve is the Raman spectrum enhanced by a factor of 10. Activation of the strong IR line is observed as a shoulder on the strong Raman line (arrow 2). The activation of the strong Raman line in the IR spectrum, conversely, is more evident (arrow 1). The simulated peaks are Lorentzian functions with a fwhm of 4 cm^{-1} .

(28) These calculations demonstrate that the effect generated by the violation of mutual exclusion is much less prominent in the Raman spectra than in the IR spectra. Thus, experimentally it is difficult to observe such a violation of mutual exclusion in the Raman spectra.

(29) See the Supporting Information for a full list of harmonic frequencies, IR and Raman intensities, and irreducible representations of the normal modes.

nicely demonstrate that the violation of mutual exclusion does not depend on the end group (i.e., adamantyl versus hydrogen),

Table 2. Vibrational Frequencies and IR and Raman Intensities of Linear ($D_{\infty h}$) and Bent (C_{2v}) Conformations of Hydrogen-End-Capped Polyynes $H-(C\equiv C)_5-H^a$

irrep ^b	frequency (cm ⁻¹)	Raman intensity (A ⁴ /amu)		IR intensity (km/mol)			
		$D_{\infty h}$	C_{2v}	$D_{\infty h}$	C_{2v}		
Σ_g^+	A ₁	2008	2008	3579	3423	0.0	0.0
Σ_u^+	B ₂	2083	2082	0.0	133	17	17
Σ_g^+	A ₁	2104	2104	39552	36432	0.0	1.0
Σ_g^+	A ₁	2180	2179	248	240	0.0	0.2
Σ_u^+	B ₂	2210	2210	0.0	348	4	4

^a Data were obtained from DFT calculations carried out at the PBEPBE/cc-pVQZ level. Data for the strongest Raman line are highlighted in bold print. ^b Irreducible representation.

Table 3. Vibrational Frequencies and IR and Raman Intensities of Adamantyl-End-Capped Polyynes **C12**, **C16**, and **C20**^a

irrep ^b	frequency (cm ⁻¹)	Raman intensity (A ⁴ /amu)		IR intensity (km/mol)	
		$D_{\infty h}$	C_{2v}	$D_{\infty h}$	C_{2v}
C12					
u	2038	12		16	
g	2066	351598		2	
g	2138	3176		0.3	
u	2205	239		279	
u	2212	356		549	
g	2242	42662		2	
C16					
g	1587	1007		0.001	
g	1977	1078980		0.2	
u	2007	1		14	
g	2092	4297		0.02	
g	2142	99		1138	
u	2163	2		57	
g	2210	4881		0	
g	2221	160367		0.3	
u	2235	33		617	
C20					
g	1619	1171		0.01	
g	1902	2670098		4	
u	1987	18		12	
g	2059	5391		0.2	
u	2079	3863		1693	
u	2124	53		62	
g	2174	300530		5	
g	2177	1568		0.04	
u	2210	4		0.01	
u	2224	1581		1380	
g	2232	140834		4	

^a Data were obtained from DFT calculations carried out at the PBEPBE/cc-pVDZ level. Data for the strongest Raman lines are highlighted in bold print. The calculations were carried out on slightly bent optimized structures (see the Supporting Information). ^b Irreducible representation deduced by approximating the symmetry of the chain as C_i (i.e., by neglecting the bending of the chain).

and they are also consistent with the results obtained with the less expensive basis set (cc-pVDZ).

Finally, DFT calculations were used to ensure that the weak band observed in the IR spectra that corresponds to the strong Raman line (see Figure 2) should not be assigned to an ungerade IR-active vibration with a similar frequency but instead to the normal mode observed in the Raman spectrum at the same frequency. The results of DFT calculations at the cc-pVQZ level for $H-(C\equiv C)_5-H$ with both linear and bent polyynes geometries (Table 2) and at the cc-pVDZ level for adamantyl-end-capped polyynes **C12**, **C16**, and **C20** with bent geometries (Table 3) were examined. The frequencies falling in the region of interest of the present study (1900–2200 cm⁻¹) were considered; for **C16** and **C20**, the first mode with a frequency smaller than the strong Raman line was also included. It should be noted that

these modes consistently show a large C—C stretching character, and the strong Raman line in these molecules can be always described as a collective, in-phase C≡C stretching coupled with the in-phase C—C shrinking (\mathcal{A} mode; see Figure 3 and ref 17b).

As shown in Table 2, none of the C≡C vibrational frequencies are affected upon moving from the linear ($D_{\infty h}$) to the bent (C_{2v}) conformation for the carbon chain in $H-(C\equiv C)_5-H$. Furthermore, these data show that no IR-active ungerade vibrations are found in the proximity of the strong gerade Raman-active vibration at 2104 cm⁻¹. Inspection of the data reported in Table 3 confirms that this is also the case for polyynes **C12**, **C16**, and **C20**, i.e., there are no IR-active ungerade vibrations found in the proximity of the strong gerade Raman active vibrations at 2066, 1977, and 1902 cm⁻¹, respectively. Thus, the DFT results confirm that in all of the cases considered, irrespective of basis-set size and chain termination, the signals observed experimentally in the solid- and solution-state IR spectra for **C16**–**C20** can be ascribed to a violation of mutual exclusion rather than to an ungerade IR vibration.

Conclusions

In summary, Raman and IR spectroscopic analyses, with the help of X-ray crystallography and DFT calculations, show that adamantyl-end-capped polyynes adopt a nonlinear (bent) structure in both the solid and solution states. This premise is confirmed by the observation in the IR and Raman spectra of a failure of the mutual-exclusion principle and the occurrence of the Raman-active \mathcal{A} -mode line in the IR absorption spectra of **C12**–**C20**. This experimental evidence is remarkable, since it suggests that a bent shape is a characteristic of the molecule itself rather than the result of external influences such as crystal packing effects. It is necessary to point out, however, that the solution-state IR and Raman data presented here cannot establish the underlying cause of the violation of mutual exclusion, so the following question remains: does the violation derive from a nonlinear equilibrium conformation(s) (static symmetry breaking), large-amplitude bending vibrations (dynamic symmetry breaking), or both? Further theoretical and experimental studies are required to shed light on the answer to this question.

Acknowledgment. In Italy, this work was supported in part by the Center of Excellence for the Engineering of Nanostructured Materials and Surfaces at the Politecnico di Milano and by grants from the Italian Ministry of Education, University and Research through FIRB project “Molecular compounds and hybrid nanostructured materials with resonant and non-resonant optical properties for photonic devices” and by PRIN project “Molecular materials and nanostructures for photonics and nanophotonics”. In Canada, this work was generously supported by the University of Alberta and the Natural Sciences and Engineering Research Council of Canada (NSERC) through the Discovery Grant program. Fellowship support from the Alberta Ingenuity Fund and NSERC (to W.A.C.) is gratefully acknowledged. The constructive criticism and suggestions of the reviewers are gratefully acknowledged.

Supporting Information Available: Synthetic details and spectroscopic characterization for **C4**–**C20**, crystallographic details and CIF files for compounds **C8** and **C12**, details about the acquisition of the Raman and IR spectra, and results of the computational simulations. This material is available free of charge via the Internet at <http://pubs.acs.org>.

JA078198B